

How Crystal Structure and Phase Segregation of Au-Fe Alloy Nanoparticles is ruled by Molar Fraction and Size

*Anna Tymoczko, Marius Kamp, Oleg Prymak, Christoph Rehbock, Jurij Jakobi, Ulrich Schürmann, Lorenz Kienle, Stephan Barcikowski**

Table of Contents

1. Experimental Section
2. Characterization of Au-Fe laser generated nanoparticles

Experimental Section

Au-Fe nanoparticles synthesis

For all studies Au-Fe alloy targets (fem Institut für Edelmetalle und Metallchemie, Schwäbisch Gmünd) with varied Au:Fe atomic % ratio (10:90, 20:80, 35:65, 50:50, 65:35, 80:20 and 90:10) were ablated in Acetone 99.98 % (Carl-Roth GmbH, Karlsruhe). LAL was performed with a 10 ns Nd:YAG laser (Rofin Sinar Technologies, Plymouth) at 1064nm with a repetition rate of 15 kHz and a fluence 3.85 mJ/cm². A lens with a focal length of 100 mm was used to focus the beam through a glass window into the batch reactor containing the Au-Fe alloy target emerged in 30 mL acetone. The alloy target was placed vertically to the bottom of the batch-chamber. Additionally, an electrical motor was mounted at the back of the chamber to assure a constant flow of the ablated material, avoiding absorption of the laser energy by already generated NPs. The amount of ablated mass was determined gravimetrically by weighting the target before and after laser ablation using a microbalance.

Particle analysis

The size and the internal composition of LAL generated Au-Fe nanoparticles were determined using transmission electron microscopy STEM-HAADF (FEI, Tecnai F30 G² STWIN). 10 µL of the colloid dispersion were pipetted onto a carbon-coated copper microgrid and dried overnight. The ferret diameter of the sample was measured for weighted 1000 nanoparticles each. The results were plotted both as number and volume-weighted distribution and fitted using a log-normal function. The average particle size was obtained from the Xc values of this fit. Energy dispersive x-ray spectroscopy is a suitable method for quantitative elemental detection of the iron gold system. Thus differentiation of the elements and corresponding oxide is distinct. EDX results are obtained by STEM-EDX measurements with Phillips XL 30 with EDAX DX-4. Therefore, different kind of EDX spectra are generated. The integration over a large number of nanoparticles confirms the coincidence of target and nanoparticle composition. Based on Z-contrast of STEM-HAADF imaging mode, a distinct hint of the ultrastructure is possible. EDX mapping and line scans characterize the existence of the CS ultrastructure in each sample. Furthermore, the absence of oxidation especially in the iron core of Au@Fe nanoparticles were proved by this method. By means of X-ray powder diffraction (XRD) using a Bruker D8 Advance diffractometer (Cu K α radiation, $\lambda = 1.54 \text{ \AA}$; 40 kV, 40 mA) a phase composition of all targets and produced Au-Fe NPs was determined. The target materials were positioned in sample holder. All nanoparticle samples were prepared from a high concentrated colloid a homogeneously distributed on a silicon single crystal to minimize scattering. To determine the phase ratios, lattice parameters and percentage of the Fe/Au substitution in the FCC and BCC structures as well as to estimate the average crystallite sizes from diffraction peak broadening reflections (using the Scherrer equation), the Rietveld refinement was performed with the Bruker software TOPAS 4.2. The patterns of cubic Au-FCC (#004-0784) and Fe-BCC (#006-0696) phases from the ICDD database were used as reference for the qualitative phase analysis, which was done with a Diffrac. suite EVA V1.2 from Bruker.

Characterization of Au-Fe laser generated nanoparticles

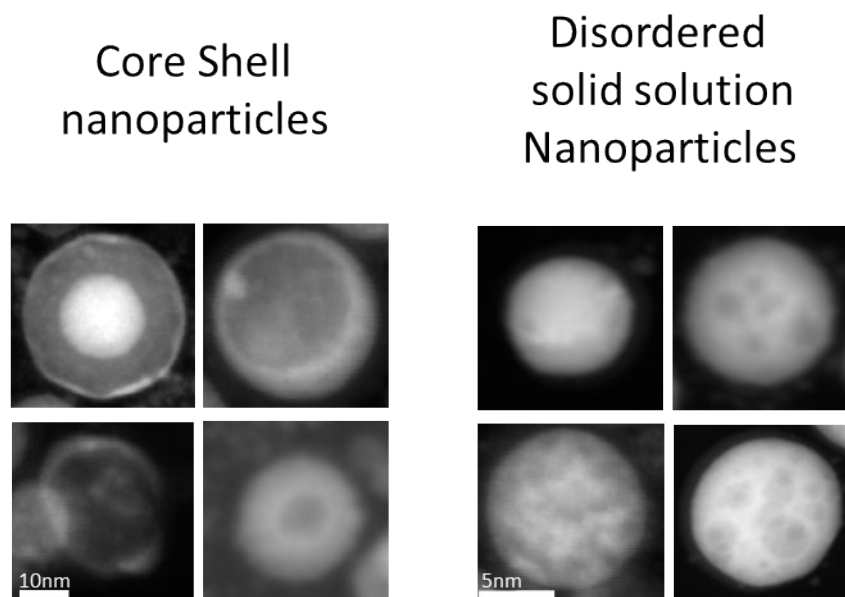


Figure S1 Representation of possible Au-Fe alloy ultrastructure generated via LAL in Acetone. The structure of Au-Fe bimetallic nanoparticle can be defined by distribution mode of the two elements and its orientation is described as a) Core Shell arrangement with clearly defined segregated Au-Fe phase boundary (Core Shell nanoparticles) b) randomly mixed alloy structure (disordered solid solution nanoparticles).

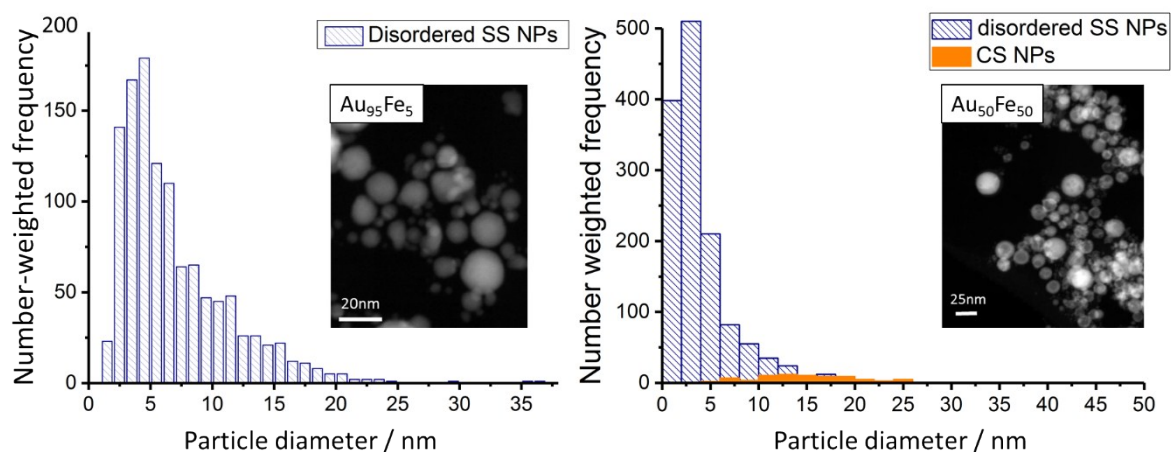


Figure S2 Two representative number-weighted particle size histograms for LAL generated $\text{Au}_{95}\text{Fe}_5$ and $\text{Au}_{50}\text{Fe}_{50}$ nanoparticles analyzed by HAADF STEM (blue bars Disordered Solid Solution NPs, orange bars Core-Shell NPs).

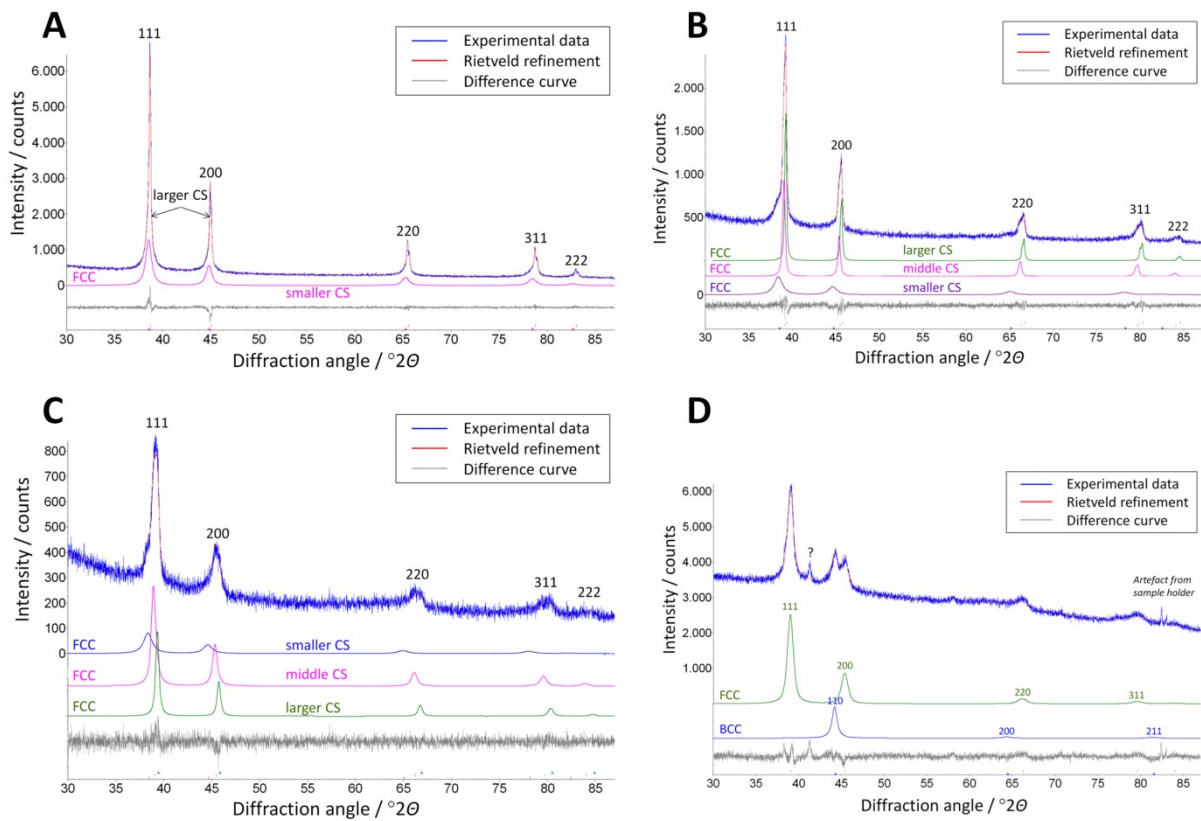


Figure S3 Representative X-ray powder diffractograms with Rietveld refinement of $\text{Au}_{80}\text{Fe}_{20}$ (A), $\text{Au}_{65}\text{Fe}_{35}$ (B), $\text{Au}_{50}\text{Fe}_{50}$ (C) and $\text{Au}_{20}\text{Fe}_{80}$ (D) nanoparticles with additionally denoted FCC and BCC phases (incl. multiply FCC peak profiles with smaller-larger crystallite sizes, CS) for the investigated Au-Fe nanoparticles. One non-identified reflection peak (?) probably belongs to Iron-oxide phase, which is observed for the Au-Fe nanoparticles with BCC-phase.